A Systematic Review of the Tensile Biomechanical Properties of the Neonatal Brachial Plexus

Virginia Orozco, MS

Drexel University 3140 Market St, BOSSONE 718 Philadelphia, PA 19104 vgo23@drexel.edu

Rachel Magee, MS

Drexel University 3140 Market St, BOSSONE 718 Philadelphia, PA 19104 rem347@drexel.edu

Sriram Balasubramanian, PhD

Drexel University 3140 Market St, BOSSONE 718 Philadelphia, PA 19104 sb939@drexel.edu

Anita Singh, PhD.1

Widener University
One University Place,
Chester, PA 19013
Telephone: (610) 498-4055
Eav: (610) 489-40059

Fax: (610) 489-40059 asingh2@widener.edu

¹Anita Singh, PhD BIO-20-1543

ABSTRACT

Brachial plexus birth injury has a reported incidence of 1 to 4 per 1000 live births. During complicated deliveries, neonatal, maternal, and other birth-related factors can cause overstretching or avulsion of the neonatal brachial plexus leading to injury. Understanding biomechanical responses of the neonate brachial plexus when subjected to stretch can offer insight into the injury outcomes while guiding the development of preventative maneuvers that can help reduce the occurrence of neonatal brachial plexus injuries. This review article aims to offer a comprehensive overview of existing literature reporting biomechanical responses of the brachial plexus, in both adults and neonates, when subjected to stretch. Despite the discrepancies in the reported biomechanical properties of the brachial plexus, the studies confirm the loading rate and loading direction dependency of the brachial plexus tissue. Future studies, possibly in vivo, that utilize clinically relevant neonatal large animal models can provide translational failure values of the biomechanical parameters for the neonatal brachial plexus when subjected to stretch.

Introduction

Despite improvements in obstetric care, brachial plexus birth injury (BPBI) continues to be reported among newborns with a worldwide incidence of 1 to 4 per 1000 live births [1-8]. BPBI results from over-stretching of the brachial plexus (BP) and/or avulsion of the BP spinal nerve roots (i.e., C5 – Th1, C: cervical and Th: Thoracic) during complicated birthing scenarios [2; 4; 7-11]. Shoulder dystocia, a birthing scenario where the fetal shoulder impacts against the mother's pubic symphysis, is strongly associated with BPBI [1-3; 8]. Other associated risk factors of BPBI can be divided into three categories: (1) neonatal, (2) maternal, and (3) birth-related. Neonatal risk factors include high birth weight (i.e., >4000 grams), which has also been strongly associated with shoulder dystocia [1-5; 8]. Maternal risk factors include age (i.e., >35 years), obesity, abnormal pelvic anatomy, gestational diabetes mellitus, and previous shoulder dystocia complication [1-5; 8]. Birthrelated risk factors include increased duration and management of labor and delivery mode (i.e., vaginal, cesarian, vacuum, or forceps) [1-5; 8]. During complicated scenarios, BPBI lesions can occur due to over-stretching of the BP nerve segments, avulsion of the spinal nerve roots, or a combination of both lesions [2; 4; 5; 7; 10; 11]. The severity of the injury is only determined after the first three months of birth, with spontaneous recovery reported in 70-90% of affected infants [4; 7; 8; 12], and permanently reduced range of motion, and decreased strength, size, and girth of the affected muscles reported in 20-30% of the affected infants [6; 9; 13]. Delayed prognosis of BPBI can be attributed to the poor understanding of the biomechanical responses of the neonate BP when overstretched during complicated deliveries.

Currently available literature on the biomechanical response of BP when stretched remains limited and variable [14-24]. The reported variability of the BP stretch response can be attributed to the anatomical complexity of the BP, tissue processing (i.e., fixed

¹Anita Singh, PhD BIO-20-1543 3

versus unfixed tissues), and variable methodology in measuring elongation of the BP tissue. Additionally, most of the reported data are based on adult human cadaveric tissue [14-20] or adult animal tissue [21-23], except for one study that utilized a neonatal piglet model [24]. Ethical limitations in obtaining biomechanical data from human neonate BP imposes the need to rely on data obtained from adult human cadaveric tissue [14-20] or animal [21-24] studies. This review article offers a comprehensive summary of published studies that have reported the tensile biomechanical responses and failure values of BP tissue when subjected to stretch. Furthermore, this review highlights the limitations of previously published studies, related research gaps, and potential future directions in the study of the neonatal BP.

Anatomy of the Brachial Plexus

BP is a complex network of nerves responsible for providing motor and sensory innervation to the upper extremities [4; 7; 8; 25]. Originating as an extension from the ventral rami of C5 through Th1 spinal nerve roots, the BP is organized into five zones, namely roots, trunks, divisions, cords, and terminal nerve branches [4; 7; 8; 25], as shown in Fig. 1. The roots are divided as the upper (i.e., C5-C6), middle (i.e., C7), and lower (i.e., C8-Th1) trunks [4; 7; 8; 25] and form the posterior and anterior divisions. The cords, formed from these divisions, are divided into lateral, medial, and posterior cords that bifurcate into the five terminal nerve branches: musculocutaneous, axillary, median, radial, and ulnar [4; 7; 8; 25].

Classification of Brachial Plexus Injury

BP injuries can be classified as neuropraxia, axonotmesis, and neurotmesis, following lesions to any of the neural structures (i.e., axons, myelin sheath) or connective tissue structures (i.e., epineurium, perineurium, endoneurium), as shown in Fig. 2 [26-31]. Neuropraxia lesions follow damage to the myelin sheath with intact axonal and connective

tissue structures (Fig. 2B) [26; 27; 30]. Axonotmesis observes axonal loss and disruption of the myelin sheath with preservation of the supporting connective tissue structures (Fig. 2C) [26; 27; 30]. Neurotmesis, the most severe injury, is characterized by a complete transection of axons, myelin sheath, and surrounding connective tissues (Fig. 2D) [26; 27; 30].

Methods

Publications included in this review were based on a Boolean search of the PubMed database with search keywords: brachial plexus, neonate, neonatal, tensile properties, biomechanical properties, mechanical properties, biomechanical testing, mechanical testing, stretch, tension, stretching, stress, and strain.

Findings

Search results from combinations of aforementioned keywords are summarized in Fig. 3A. After excluding non-English results, remaining search results were screened for eligibility, and duplicate studies were removed. Published studies (1986 to 2020) eligible for this review examined the failure tensile biomechanical properties of the BP in both human and animal models, and reported parameters such as failure load, stress, strain, and elastic modulus (Fig. 3B). Eleven relevant articles in the English-language were included in this review paper. Seven of these studies used fixed and unfixed adult human cadaveric tissue [14-20], four studies utilized animal models, of which three studies used adult animal models [21-23], and one used a neonate animal model [24].

Overview of Biomechanical Responses in Peripheral Nerves During Stretch

Several studies on peripheral nerves have shown the biomechanical response to be related to the type of nerve fiber injury [26], the proportion of the number of fascicles between nerves [32], injury to either surrounding connective tissue structures [26; 32], and testing methodologies (i.e., loading rate, loading direction) [14-24; 33; 34]. Studies have

shown stretching of a nerve can result in perineural damage while the nerve appears grossly intact [32; 35]; furthermore, damage can also occur at multiple sites; therefore, gross inspection may not accurately identify the level of injury [32; 35]. In addition, nerves have been shown to exhibit viscoelastic properties, which protect the nerves during normal range of motion [32; 35] and help keep the structural integrity of the nerve fibers [32]. Therefore, it is critical to differentiate between biomechanical responses of nerves during normal range of motion versus injury both at slow- and rapid-loading rates (i.e., failure biomechanics). Limited information is available on the neonatal BP biomechanical properties, which is critical to further our understanding of the injury mechanism of BPBI.

Tensile testing of peripheral nerves has been performed to quantify its biomechanical response during stretch [26; 32; 35; 36]. A known force or known elongation is applied, while the elongation or force of the specimen is measured, respectively [36]. A typical load-elongation curve obtained from such testing is shown in Fig. 4A. The obtained load-elongation data is used to report biomechanical properties including: (1) maximum load [N] (highest peak on the load-displacement curve), (2) strain [%] (calculated by dividing the change of length over the original length), (3) stiffness [N/mm] (calculated slope of the linear region of the load-elongation curve), (4) stress [MPa] (calculated by dividing the load over the cross-sectional area of the tissue), and (5) elastic modulus [MPa] (calculated slope of the linear region of the stress-strain curve) (Fig. 4A and 4B).

In vitro BP Studies in Adult Cadaveric Tissue

Current literature on tensile biomechanical response of human BP tissue is limited to adult human cadaveric tissue [14-20]. Destandau et al., 1986 stretched 48 intact cervical spinal nerve roots obtained from fresh human cadavers at a rate of 600 mm/min until mechanical failure occurred using a tensile testing device (Unité 103, INSERM, French National

¹Anita Singh, PhD BIO-20-1543 6

Institute of Health and Medical Research) [14]. Individual spinal nerve roots (n = 48, two spinal nerve roots not included because of length and dissection error) from 10 anterior branches of five fresh spines were stretched (Fig. 5A) [14]. The observed biomechanical response from the load-displacement curve began with an ascending slope defining the elastic region until a maximum peak force was observed (i.e., mechanical failure of the tissue), which was then followed by a descending slope due to subsequent gross ruptures of the tissue from its attachments [14]. The average rupture force for each BP spinal nerve root is shown in Fig. 5B. Avulsion-type injuries were reported in 16 out of 48 spinal nerve roots at an average rupture force of 69.3 ± 27.8 N, and non-avulsion rupture-type injuries were reported in the remaining 32 spinal nerve roots at an average rupture force of 79.3 ± 26.3 N (Fig. 6). Furthermore, spinal nerve roots C8 (6/16) and Th1 (6/16) avulsed more frequently compared to other spinal nerve roots (C5 (1/16), C6 (2/16), and C7 (1/16)) [14]. The C5, C6, and C7 spinal neve roots were found to be more resistant to avulsion-type injuries, compared to C8 and Th1 spinal nerve roots (Fig. 7A), because the dura mater and foraminal connections (i.e., protection mechanism of spinal nerves against stretch) are stronger [14]. The average rupture force of avulsion and non-avulsion injury-type of each BP spinal nerve root is shown in Fig. 7B.

In another study, Ma et al., 2013 studied the *in vitro* mechanical properties of the human ulnar (n = 4) and median (n = 2) nerves that are BP terminal nerve branches [18]. Fresh nerves were harvested and stretched at a rate of 3 mm/min. Both ends of the nerves were clamped with one end attached to a load cell (LSB200 Miniature S Beam, FUTEK Advanced Sensory Technology, Irvine, CA) and the other to a motorized linear translation stage (MTS25X, THORLABSS, Newton, NJ). The study reported *in vitro* mechanical properties of the ulnar and median nerves to be comparable and highly hyperelastic and viscoelastic [18].

Effect of Loading Rate

Loading rate-dependency of BP tissue properties has also been investigated in human cadaveric studies. Marani et al., 1993 reported the mechanical response of formalin-fixed (n = 20) and unfixed (n = 2) adult human cadaveric BP tissue subjected to stretch at varying loading rates using a tensile testing machine (Hounsfield HT, England). A total of 16 BP tissues were clamped at both ends and stretched to mechanical failure at the following rates: 10 mm/min, 20 mm/min, 50 mm/min, and 500 mm/min [15]. Two formalinfixed and two unfixed BP tissues were tested at each of the four rates. Rupture was observed mostly at the moving clamp side. The biomechanical response of formalin-fixed and unfixed BP tissue also exhibited an initial ascending slope describing the elastic region followed by maximum force and then descending stepwise slope during rupture. The observed response was similar to that reported by Destandua et al., 1986 in BP spinal nerve roots [14; 15]. The authors attributed the stepwise slope after maximum force to represent ruptures of individual nerve fibers, which suggest subsequent perineurial sheaths resisted rupture separately after the initial epineural rupture [15]. The authors also found the mechanical work for total rupture of the tested BP tissue to be twice the initial rupture value [15]. Furthermore, at lower rates, nerves elongated up to one-third of their resting length before rupture as compared to faster rates where elongation reduced to 1/30th or 1/20th of the resting length of the nerve before rupture [15]. The effect of formalinfixed versus unfixed BP nerve tissue biomechanical responses are discussed in a later section.

Effect of Loading Direction

Given that injury to the BP complex can be observed as either spinal nerve root avulsion, nerve rupture, or a combination, studying the entire BP complex (often referred to as intact) under mechanical stretch in varying loading directions, is necessary. A few human

cadaveric studies have investigated the effect of loading direction on intact BP complexes during mechanical stretch to confirm that loading direction directly influences the failure site [16; 17; 19].

Zapalowicz et al., 2000 reported that a direct lateral traction resulted in predominantly avulsion-type injures of intact BP complexes [16]. Eleven fresh, intact BP complexes (three unilateral and four bilateral) from seven adult human cadavers, with no history of neurological disease, were harvested after isolating them from the surrounding muscles and connective tissues, and after cutting the BP terminal nerve branches at the axilla [16]. The intact BP complexes were then stretched to complete rupture at a rate of 10 mm/min using a tensile testing apparatus (INSTRON, Norwood, MA). The BP terminal nerve branches were clamped at the moving end of the tensile testing apparatus, and the spinal column was secured such that the pulling force was in the lateral direction. Out of the 11 stretched intact BP complexes, the initial injury occurred twice C5, once at C5 and C6, once at C7, thrice at C8, once at C8 and Th1, once at the upper trunk, and twice at the cords. For avulsion-type injures of intact BP complexes pulled in a direct lateral traction, the reported average rupture force was 388.5 N (range: 217.7-546.3 N), average rupture stress was 2.6 MPa (range: 1.3–3.5 MPa), and average elongation at rupture was 38.6% (range: 19.6-58.8%) [16]. It was observed that a direct lateral traction led to predominantly avulsion-type injury that started from the anterior margin of the epineurium tearing it away from the intervertebral foramen. The authors postulated that the anterior margin of the epineural attachment was more susceptible to tearing away from the intervertebral foramen in comparison to the posterior margin because of the weakened bindings between the transverse processes [16].

In another study, Zapalowicz et al., 2005 used 30 fresh human intact BP specimens obtained from 15 adult cadavers (average age 38 years, range 19–55 years)

¹Anita Singh, PhD BIO-20-1543 9

that were divided into three groups. Each group had ten intact BP complexes that were stretched at three distinct loading directions (45° caudal, perpendicular, parallel with respect to the midline of the spinal column) until mechanical failure at a rate of 200 mm/min using an INSTRON 4000 (INSTRON, Norwood, MA) testing apparatus [17]. Similar to their previous study [16], the BP terminal nerve branches were clamped at the moving end of the testing apparatus and the spinal column was positioned and secured such that pulling force was 45° caudal (Group 1), perpendicular (Group 2), or parallel (Group 3). As reported by Destandua et al., 1986 in BP spinal nerve roots and Marani et al., 1993 in BP nerve tissue, this study also demonstrated an initial ascending slope, followed by maximum force and then a descending slope that characterized the intact BP complex load-displacement response when stretched [14; 15; 17]. Loading force direction did not have an effect on the biomechanical response; however, the authors reported loading force direction influenced the initial injury-type (avulsion- or rupture-type) of intact BP complexes. Of the 30 intact BP specimens, a total of 70 initial lesions were identified where 22, 26, and 22, occurred in Group 1, Group 2, and Group 3, respectively [17]. In the 45° caudal load pulling direction (Group 1, n = 22), nine avulsions (9/22, 41%) and 13 ruptures (13/22, 59%) were observed at the failure force. When stretched perpendicular to the midline of the spine (Group 2, n = 26), 23 avulsions (23/26, 88%) and three ruptures (3/26, 12%) were observed, and when stretched parallel to the midline of the spine (Group 3, n = 22), four avulsions (4/22, 18%) and 18 ruptures (18/22, 82%) were observed, as first lesion types at failure force (Fig. 8) [17]. While the authors did not report the failure forces and strains with respect to loading direction, they did report the average failure force and average elongation of intact BP complexes to be 630 N (range: 365-807 N) and 37% (range: 23–53.5%), respectively.

The authors postulated that the loading direction directly influenced the variable forces that were experienced by the epineurium of the cervical spinal nerve roots and transverse vertebral processes [17; 37] such that stretching intact BP complexes perpendicular to the loading force (Group 2) weakened the bindings between the epineurium and transverse processes, thereby making the intact BP complex more susceptible to avulsion-type injuries at the spinal nerve roots [17; 37]. In Groups 1 and 3, BP complexes were more resistant to avulsion-type injuries because the bindings between the epineurium and transverse processes pressed together, thus resisting avulsion-type lesions, but weakening the nerves that extended from the spinal nerve roots resulting in more rupture-type lesions [17].

In a more recent study, Zapalowicz et al., 2018 stretched 30 fresh intact adult human cadaveric BP complexes (average age 38 years, range 19–55 years) in three different loading directions (45° caudal, perpendicular, parallel with respect to the midline of the spinal column) until failure at a rate of 200 mm/min using an INSTRON 4000 (INSTRON, Norwood, MA) tensile testing machine [19]. All 30 specimens were equally divided into the three groups (n = 10), and the loading force was applied in a 45° caudal direction (Group A), perpendicular direction (Group B), or parallel direction (Group C), as shown in Fig. 9A. The reported average maximum force for BP failure in Group A, Group B, and Group C were $665.0 \pm 83.9 \text{ N}$, $588.0 \pm 115.7 \text{ N}$, and $632.0 \pm 85.8 \text{ N}$, respectively (Fig. 9B). No strain data were reported.

From the 30 tested intact BP complexes, a total of 89 avulsion-type and 51 rupture-type injuries were observed (a total of 140 lesions) [19]. As reported in their previous 2005 study, intact BP complexes pulled with loading force perpendicular to the spinal column's midline (Group B) observed the most avulsion-type injuries (41/89, 46%) [17; 19]. Spinal nerve roots C6 (10/41, 24.3%) and C7 (10/41, 24.3%) avulsed most frequently with a

perpendicular loading direction [19]. From the total avulsion-type injures in the three tested groups, spinal nerve roots C7 (20/89, 22.5%), C8 (20/89, 22.5%), and Th1 (20/89, 22.5%) avulsed most frequently (Fig. 10A) [19]. These findings are similar to those reported by Destandau et al., 1986, who also reported more frequent avulsion injuries of spinal nerve roots C8 (6/16, 37.5%) and Th1 (6/16, 37.5%) even at an increased loading rate of 600 mm/min [14]. Most rupture-type injuries were observed in Group A (24/51, 47%), followed by Group C (19/51, 37%), and then in Group B (8/51, 16%) [19]. In Groups A and C, rupture occurred at either the divisions (10/24, 42%, 7/19, 37%, respectively) or cords (9/24, 37.5%, 38/51, 74.5%, respectively) [19]. Overall, rupture lesions most frequently occurred at either the divisions or cords (38/51, 74.5%) and not the anterior rami or trunks (13/51, 25.5%) (Fig. 10B) [19].

These studies demonstrate a direct correlation between loading direction and the observed initial anatomical lesion [17; 19]. The studies also confirm that the observed biomechanical response of intact BP complexes are similar among the three distinct loading directions while initial lesion site differs, which the authors attribute to the binding of the epineurium and transverse process [17; 19].

Effect of Fixation

Feasibility and time constraints associated with biomechanical testing of fresh human cadaveric tissues warrant preservation of the tissue. However, fixation can affect the biomechanical responses of the studied tissue. Two studies have reported the effect of fixation, as well as type of fixation on the tensile properties of BP nerve tissue.

Marani et al., 1993 performed tensile testing on formalin-fixed and unfixed adult human cadaveric BP tissue at varying loading rates. It was found that formalin-fixed BP nerves better resisted the forces needed for rupture compared to unfixed BP nerves [15]. The reported stress values of formalin-fixed and unfixed BP nerves were 0.25 MPa and

0.14 MPa, respectively. The authors further found that both formalin-fixed and unfixed BP tissue did not show differences in their elongation responses [15].

In contrast to Marani's study, a more recent study by Stouthandel et al., 2020 reported no effect of Thiel (i.e., a soft embalming technique used to maintain the natural feel and look of tissue) fixation on the tensile biomechanical response of the median nerve, a BP terminal nerve [38; 39]. Nine (six female and three male) adult human cadavers (78 \pm 17 years old) were used. Before Thiel fixation, the median nerve of either the left or right wrist (chosen randomly) was harvested. Then, after Thiel fixation, the median nerve of the contralateral arm was harvested. Using an INSTRON 5994 with a static load-cell of 500 N (INSTRON, Norwood, MA) testing machine, the median nerves were stretched to failure at a strain rate of 0.5% per second [20]. The reported average Young's modulus values of Thiel-fixed and unfixed and median nerves were 7.45 \pm 3.40 MPa and 9.20 \pm 1.20 MPa, respectively (Fig. 11A) [20]. Using a paired Wilcoxon signed-rank test, the authors found that Thiel-fixed and unfixed median nerves did not significantly differ in elasticity (V = 10, p = 0.313) [20]. Also, similar stress-strain responses between the Thiel-fixed and unfixed median nerves (Fig. 11B) were reported, demonstrating Thiel fixation did not alter the underlying biomechanical response [20].

Summary of in vitro BP Studies in Adult Cadaveric Tissue

In summary, the available studies (Table 1) using human cadaveric BP tissue offer some understanding of the biomechanical properties of BP tissue when stretched to failure, such as:

- BP spinal nerve roots C8 and Th1 avulse more frequently than the C5 and C6 spinal nerve roots [14; 19].
- BP failure threshold varies considerable with average failure force ranging from
 69.3 N to 807 N, average failure stress from 0.14 MPa to 3.5 MPa, average strain

- at failure force from 19.6% to 58.8%, and average elastic modulus from 7.45 MPa to 9.20 MPa [14-20].
- BP tissues exhibit rate dependency such that increasing loading rate corresponds to higher failure forces [15-17].
- Loading direction influences initial injury-type (avulsion vs rupture) in intact BP complexes such that avulsion-type injuries occurs more frequently in lateral [16] and perpendicular loading direction [17; 19], compared to 45° caudal and parallel loading direction, which results in more rupture-type injuries [17; 19].
- Type of fixation may have an effect on the biomechanical properties of BP nerves
 [15; 20].

In vitro BP Studies in Adult Animal Models

A few studies have investigated biomechanical responses of the BP complex using adult animal models. Kawai et al., 1989 performed stretch studies on the BP of adult rabbits (n = 19) at three distinct loading directions (upward, lateral, downward) until mechanical failure. To identify the stress and strain needed for an avulsion- or rupture-type lesions of the BP, the C6 nerve root level of six out of the 19 adult rabbits were isolated from the other nerve roots and stretched laterally (n = 3) for avulsion-type injury and downward (n = 3) for rupture-type injury at a rate of 500 mm/min using an axial-loading testing apparatus with a graphic recorder (Shimadzu Autograph S-500-C, Shimadzu, Kyoto, Japan). The C6 nerve root avulsion average failure stress and strain were reported to be 26 MPa (range: 23–27 MPa) and 9%, respectively; while the average failure stress and strain for C6 nerve root rupture were 46 MPa (range: 44–49 MPa) and 7%, respectively [21]. The observed average failure stress was twice as much for a C6 rupture-type injury than a C6 avulsion-type injury, while the reported strains at failure were similar. The authors attributed the observed difference in the failure stress between avulsion- and rupture-type injuries to the lack of perineurium, a nerve structure that most resists over-stretching, in the nerve roots

[21]. The effect of loading direction on the BP biomechanical responses reported in this study is discussed in a later section.

In another study, Takai et al., 2002 performed tensile testing on the lower BP trunk of adult rabbits. The lower BP trunks of adult rabbits (n = 6) were isolated, dissected free, anchored to an axial tensile testing set-up (Shimadzu Autograph AGS-500B, Shimadzu, Kyoto, Japan), and stretched to failure at a rate of 10 mm/min [22]. The reported average values for maximum tensile force, ultimate tensile stress, ultimate strain, and elastic modulus were $16.9 \pm 2.7 \text{ N}$, $6.9 \pm 0.39 \text{ MPa}$, $24.0 \pm 1.1\%$, and $28.5 \pm 1.8 \text{ MPa}$, respectively [22].

Phillips et al., 2004 also performed tensile testing on median and sciatic nerves obtained from joint and non-joint sections of an adult rat animal model to identify if regional differences (i.e., joint versus non-joint nerve sections) existed in the biomechanical properties of the nerve [23]. Using a Testometric 220M (Testometric Co Ltd, Rochdale, UK), the samples were stretched until failure at a rate of 10 mm/min. Although failure tensile properties were not reported directly, the authors reported a stiffness ratio (i.e., stiffness of joint specimen divided by the stiffness of non-joint specimen). For the median and sciatic nerve, the average stiffness ratio was less than 1 (i.e., 0.5 ± 0.07 and 0.8 ± 0.02 , respectively) [23]. The authors concluded that nerve regions near the joint to be more compliant compared to nerve regions farther away from the joint (i.e., stiffer nerve regions farther away from the joint) [23]. This finding further adds complexity to understanding the biomechanical properties of the BP peripheral nerves, since heterogeneity contributes to variations in tensile biomechanical responses.

Effect of Loading Direction

Similar to the previously reported studies in *in vitro* human cadaveric studies [16; 17; 19], animal studies also reported loading direction to influence the injury type of intact BP

complexes. Kawai et al., 1989 performed stretched 13 intact BP complexes using an adult rabbit animal model at three distinct loading directions (upward (n = 5), lateral (n = 5), and downward (n = 3)). The BP complexes of euthanized rabbits were explored and isolated, such that the upper limb was connected to the neck only by the BP [21]. Intact BP complexes (upward (n = 5), lateral (n = 5), and downward (n = 3)) were stretched to mechanical failure at a rate of 500 mm/min for each loading direction using an axial-loading apparatus with a graphic recorder (Shimadzu Autograph S-500-C, Shimadzu, Kyoto, Japan) [21].

Average failure force was 20 N (range: 16–23 N) in upward loading direction, 23 N (range: 19–31 N) in lateral loading direction, and 38 N (range: 36–39 N) in downward loading direction (Fig. 12) [21]. In both upward and lateral loading directions, a combination of avulsion- and rupture-type lesions were observed, with avulsion injuries being more frequent. In these two loading directions, all C5 nerves were rupture-type lesions, C6–C8 were all avulsion-type lesions, and Th1 observed 7/10 (70%) avulsions and 3/10 (30%) ruptures [21]. When stretched upward and lateral, spinal nerve root Th1 failed first, followed by C8, C7, C6, and C5 spinal nerve root levels. In the downward loading direction, rupture-type injuries were predominantly observed [21]. Similar to the findings of Zapalowicz et al., 2005 and 2018, Kawai et al., 1989 also reported loading direction to influence the type of injury observed (avulsion versus rupture injury-type) [17; 19; 21].

Effect of Loading Rate

No study has reported the effect of loading rate on BP tissue properties using adult animal models.

Summary of in vitro BP Studies in Adult Animal Models

The reported *in vitro* biomechanical properties of the BP in adult animal models (Table 2), provides an understanding of the biomechanical properties of the BP, such that:

- BP spinal nerve roots C6, C7, C8, and Th1 avulse more frequently than C5, which primarily undergoes rupture-type injuries [21].
- The reported BP failure thresholds varies considerably such that the average failure force ranges from 16 N to 39 N, average failure stress from 6.9 MPa to 49 MPa, and average failure strain from 7% to 24% [21-23].
- Differences in species affects the tissue response because of variation of BP tissue dimensions such as size, diameter, length, and fiber pattern, as well as spinal nerve roots defining the BP [40; 41].
 - Anatomical exploration revealed rabbit BP extends from spinal nerve roots C5, C6, C7, C8, Th1, and Th2 (sometimes) and has an upper and lower trunk; while the rat BP extends from C5, C6, C7, C8, and Th1 spinal nerve roots and has an upper, middle, and lower trunk [41].
- Similar to *in vitro* human studies [16; 17; 19], loading direction influences the injury-type of intact BP complexes, such that upward and lateral stretch result in a combination of avulsion- and rupture-type injuries with avulsion injuries being more frequent, while downward stretch result in mainly rupture-type injuries [21].
- Effects of loading rate is not yet addressed in the available adult animal studies.

In vitro BP Studies in Neonatal Animal Model

Biomechanical responses of the neonatal BP are needed to manage the occurrence of BPBI. However, a serious limitation is the lack of biomechanical data from neonatal human BP tissue. Ethical limitations with performing studies on human neonatal tissue warrant new approaches that can help investigate neonatal BP tensile biomechanical responses. Studies employing neonatal large animal models can serve as promising surrogates.

Following an extensive search for this comprehensive review article, Singh et al., 2018 was the only study to report the tensile biomechanical properties of neonatal BP tissue in 3-5 days old neonatal piglets [24].

Effect of Loading Rate

Neonate piglet BP segments (root/trunk, cord, and terminal branches, n = 114), as well as the tibial nerve (n = 11) from the same animals, were subjected to quasi-static (0.6 mm/min) and dynamic (600 mm/min) displacement rates until failure using an ADMET material testing machine (eXpert 7600, ADMET Inc., Norwood, MA) [24]. At quasi-static rate, average maximum force, maximum stress, maximum strain, and elastic modulus of the neonatal BP complex were 1.83 \pm 0.14 N, 0.56 \pm 0.07 MPa, 0.32 \pm 0.03, and 2.87 \pm 0.32MPa, respectively [24]. In contrast, average maximum force, maximum stress, maximum strain, and elastic modulus at the dynamic rate were 3.52 ± 0.42 N, 1.15 ± 0.15 MPa, 0.32 ± 0.02, and 5.27 ± 0.69 MPa, respectively [24]. The study further observed that BP terminal nerve segments failed at higher stresses than BP cord and root/trunk segments at both rates [24]. When comparing biomechanical properties between BP terminal nerve segments and tibial nerves at both rates, no significant differences were found [24]. However, significantly higher maximum stresses and modulus were measured in tibial nerves compared to BP root/trunk and cord segments at both rates [24]. Among BP segments and between BP segments and tibial nerve, no significant difference in strain values were reported [24].

Effect of Loading Direction

No study has reported the effect of loading direction in neonatal BP tissue using a neonatal animal model.

Summary of in vitro BP Studies in Neonatal Animal Model

Biomechanical studies in a piglet animal model (Table 3) provides an understanding of the biomechanical properties of the neonatal BP, such that:

- At a quasi-static rate (0.6 mm/min), average maximum force, maximum stress, maximum strain, and elastic modulus are 1.83 ± 0.14 N, 0.56 ± 0.07 MPa, 0.32 ± 0.03, and 2.87 ± 0.32MPa, respectively [24].
- At a dynamic rate (600 mm/min), average maximum force, maximum stress, maximum strain, and elastic modulus are 3.52 ± 0.42 N, 1.15 ± 0.15 MPa, 0.32 ± 0.02, and 5.27 ± 0.69 MPa, respectively [24].
- Effects of loading direction is not addressed in the available neonatal animal studies.

Conclusion

Preventative obstetric maneuvers during complicated birth deliveries to help reduce occurrence of BPBI in infants can benefit from understanding the biomechanical response of the neonatal BP when stretched to failure. However, current reported biomechanical properties of BP vary due to age discrepancy, anatomical complexity, and variability in testing methodology.

Current *in vitro* BP studies in adult humans have reported average failure force ranges from 69.3 N to 807.0 N, average failure stress from 0.14 MPa to 3.5 MPa, average failure strain from 19.6% to 58.8%, and average elastic modulus from 7.45 to 9.20 MPa [14-20]. In comparison, studies using *in vitro* adult animal models have reported average failure forces ranging from 16 N to 39 N, average failure stress from 6.9 MPa to 49 MPa, and average failure strain from 7.0% to 24.0% [21-23]. The variation among the reported failure responses between *in vitro* adult human cadaveric and adult animal model studies can be attributed to differences in the testing methodologies such as employed loading rate and loading direction, and differences between the BP tissue dimensions (i.e., length,

diameter) as well as structures (i.e., fascicular pattern and spinal nerve roots involved) [40-42]. Despite the observed variations in the failure values, the stress-strain behavior observed in these studies are similar. Moreover, the reported injury types including predominant rupture-type injures of C5 and C6 BP nerve roots are also similar between the reported *in vitro* human and animal studies. These findings also align with the most commonly reported BPBI injury called Erb's palsy that is associated with injury at the junction of C5-C6 nerve roots [43].

Factors including loading rate and direction were also investigated in the reported studies. The effect of loading rate is particularly important; Allen et al., 1991 reported that as the peak force rate (in N/sec) increased, the peak force (in N) increased as observed during routine delivery, difficult delivery, and shoulder dystocia delivery [41]. Available human cadaveric studies have reported higher loading rates to result in higher failure forces within the BP tissue [15-17]. While no adult animal studies have investigated the effect of loading rate in BP tissue, Singh et al., 2006 and 2017 and Mahan et al., 2019 have also reported similar loading rate effects in the rat lumbar spinal nerve roots and sciatic nerves, respectively [44-46].

Additionally, understanding how loading direction affects neonate BP mechanical response is critical to help alleviate a stretch-induced injury resulting from a shoulder dystocia event. Using computational modeling, Gonik et al., 2003 found that downward lateral displacement of the fetal head increased BP stretch injury by 30% (18.2% BP strain) while axial positioning of the fetal head reduced BP stretch injury (14.0% BP strain) [47]. Reviewed human cadaveric and adult animal studies in BP have also confirmed a direct correlation between loading direction and resulting injury-type such that lateral, perpendicular and upward stretches result in more avulsion type injuries [16; 17; 19; 21] when compared to parallel and downward stretches [17; 19; 21].

Overall, available studies, both animal and human, offer valuable insights that help understand the effect of loading rate and loading direction on the BP biomechanical responses. The biomechanical data available from these reported studies have been utilized in existing physical and computational models to simulate complicated birthing scenarios and currently offer insight into BP stretch conditions and parameters that lead to BPBI [47-49].

Despite these available studies that report biomechanical responses of stretched BP, a major limitation is the lack of available data from human neonate BP tissue. An in vitro human study in another peripheral nerve (i.e., sciatic) reported the ultimate stress (in kg/mm²) to be greater in adults (age range: 20-69 years, 1.28 ± 0.016 kg/mm²) compared to adolescents (age range: 0-19 years, 1.14 ± 0.035 kg/mm²) and neonates (age range: one month, 0.96 ± 0.026 kg/mm²), clearly demonstrating the age-dependent differences in the peripheral nerves [50]. Ethical limitations as well as lack of transparency when evaluating and referring a potential neonatal donor have contributed to the infrequent incidence of neonatal organ and tissue donation, thereby adding to the currently unavailable data on human neonatal BP tissue [51]. An alternative could be a clinically relevant neonatal large animal model, such as a piglet. Although anatomical differences exist between piglet and human neonate BP, such as the less developed divisions between the three trunks and cords and lack of a clavicle in piglets, piglet and human neonate share similarities in BP anatomy that include origination from an upper (i.e., C5-C6), middle (i.e., C7), and lower (i.e., C8-Th1) BP segments [52]. Using a neonatal piglet animal model, Singh et al., 2018 reported the biomechanical response of BP segments and effects of loading rate on BP failure. Variation in loading rate is confirmed between various birthing scenarios such that as the difficulty of delivery increases, the loading rate increases [53]. Obtained data in a neonatal large animal model can be used to understand

the BPBI injury mechanisms under the assumption that as the loading rate for delivery increases in complicated delivery scenarios, the loading rate on the neonate BP may also increase and thus increase the likelihood of a stretch injury [24]. The study also reported that the BP terminal nerve was similar to that of a different peripheral nerve (i.e., tibial nerve) from the same animal model, but demonstrated significantly higher maximum stresses and modulus when compared to the BP root/trunk and cord segments [24]. This study was the first to report varying biomechanical properties of individual neonate BP segments (i.e., root/trunk, cord, and terminal branches) relative to each other and another peripheral nerve (i.e., tibial nerve). One major limitation, however, of this study is the lack of data on the effect of loading direction, in this clinically relevant animal model, warranting future studies to fill this critical gap.

The obtained biomechanical data from animal and human studies are and can be utilized in existing and future computational models, respectively, of maternal pelvis and neonate that simulate complicated delivery scenarios and help provide insight into biomechanical responses of BP tissue [35, 36]. Currently available computational models that help investigate the effect of clinician- and maternal-applied forces on the human neonate BP during various birthing scenarios utilize the biomechanical response of an adult rabbit tibial nerve (ultimate strain and ultimate stress are $38.5 \pm 2.0\%$ and 11.7 ± 0.7 MPa, respectively, at a rate of 10 mm/min [54]) rather than that of a neonate BP [47; 49]. Takai et al., 2002 reported an ultimate strain and ultimate stress of $24.0 \pm 1.1\%$ and 6.0 ± 0.13 MPa, respectively, at a rate of 10 mm/min of the lower BP trunk of adult rabbits [22]. Within the same species and at the same loading rate, the biomechanical response of the tibial nerve and BP differs such that tibial nerve exhibited more compliance compared to the BP [28]. This implies that computational models using the biomechanical response of a tibial nerve may not fully capture the BP response during complicated birthing scenarios.

Journal of Biomechanical Engineering

Data obtained from studies investigating *in vivo* BP responses in a neonatal large animal models would be ideal to enhance the biofidelity of the existing computational models. Furthermore, extending these *in vivo* studies to investigate effects of loading rate and loading direction in a neonatal large animal model can fill existing gaps, offer in-depth understanding of the neonate BP's biomechanical response during complicated birthing scenarios, and help obstetricians develop preventative measures, thereby advancing the science of neonatal care.

Acknowledgment

Funding

This publication was supported by funding from the Eunice Kennedy Shriver National Institute of Child Health and Human Development of the National Institutes of Health under Award Number R15HD093024 and NSF CAREER grant Award #1752513.

References

- [1] Andersen, J., Watt, J., Olson, J., and Van Aerde, J. 2006. "Perinatal brachial plexus palsy." Paediatr Child Health, **11**(2), pp. 93-100.
- [2] Zafeiriou, D. I., and Psychogiou, K. 2008. "Obstetrical Brachial Plexus Palsy." Pediatric Neurology, **38**(4), pp. 235-242.
- [3] Heise, C. O., Martins, R., and Siqueira, M. 2015. "Neonatal brachial plexus palsy: a permanent challenge." Arq. Neuro-Psiquiatr., **73**(9), pp. 803-808.
- [4] Abzug, J. M. M. D., and Kozin, S. H. M. D. 2010. "Current Concepts: Neonatal Brachial Plexus Palsy." Orthopedics (Online), **33**(6), pp. 430-435.
- [5] Romana, M., and Rogier, A. 2013. "Obstetrical brachial plexus palsy." In *Handbook of Clinical Neurology*, 921-928. Elsevier.
- [6] Nikolaou, S., Liangjun, H., Tuttle, L. J., Weekley, H., Christopher, W., Lieber, R. L., and Cornwall, R. 2014. "Contribution of denervated muscle to contractures after neonatal brachial plexus injury: not just muscle fibrosis." Muscle & nerve, 49(3), pp. 398-404.
- [7] Abid, A. 2016. "Brachial plexus birth palsy: Management during the first year of life." Orthopaedics & Traumatology: Surgery & Research, 102(1, Supplement), pp. S125-S132.
- [8] O'Berry, P., Brown, M., and Phillips, L. a. 2017. "Obstetrical Brachial Plexus Palsy." Current Problems in Pediatric and Adolescent Health Care, **47**(7), pp. 151--155.
- [9] Mehlman, C. T. 2015. "Neonatal Brachial Plexus Palsy." In *The Pediatric Upper Extremity*, edited by Joshua M. Abzug, Scott H. Kozin and Dan A. Zlotolow, 589-605. New York, NY: Springer New York.
- [10] Al-Qattan, M. M., El-Sayed, A. A. F., Al-Zahrani, A. Y., Al-Mutairi, S. A., Al-Harbi, M. S., Al-Mutairi, A. M., and Al-Kahtani, F. S. 2009. "NARAKAS CLASSIFICATION OF OBSTETRIC BRACHIAL PLEXUS PALSY REVISITED." J. Hand Surg.-Eur. Vol., **34E**(6), pp. 788-791.
- [11] Johnson, E. O., Troupis, T., Michalinos, A., Dimovelis, J., and Soucacos, P. N. 2013. "Obstetrical brachial plexus palsy: lessons in functional neuroanatomy." Injury, 44(3), pp. 293-298.
- [12] Addas, B. M. 2010. "Obstetric brachial plexus injury." Neurosciences, **15**(2), pp. 136-137.
- [13] Heise, C. O., Siqueira, M. G., Martins, R. S., and Gherpelli, J. L. D. 2009. "Motor nerve-conduction studies in obstetric brachial plexopathy for a selection of patients with a poor outcome." JBJS, 91(7), pp. 1729-1737.
- [14] Destandau, J., Micallef, J., and Rabischong, P. 1986. "An experimental study of traction on the cervical spinal nerves." Surgical and Radiologic Anatomy, 8(3), pp. 197.
- [15] Marani, E., van Leeuwen, J. L., and Spoor, C. W. 1993. "The tensile testing machine applied in the study of human nerve rupture: a preliminary study." Clinical Neurology and Neurosurgery, **95**(SUPPL.), pp. 33--35.
- [16] Zapałowicz, K., and Radek, A. 2000. "Mechanical properties of the human brachial plexus." Neurologia i neurochirurgia polska, **34**(6 Suppl), pp. 89-93.
- [17] Zapalowicz, K., and Radek, A. 2005. "Experimental investigations of traction injury of the brachial plexus. Model and results." Ann Acad Med Stetin, **51**(2), pp. 11--14.
- [18] Ma, Z., Hu, S., Tan, J. S., Myer, C., Njus, N. M., and Xia, Z. 2013. "In vitro and in vivo mechanical properties of human ulnar and median nerves." J. Biomed. Mater. Res. Part A, **101**(9), pp. 2718--2725.

- [19] Zapałowicz, K., and Radek, M. 2018. "The distribution of brachial plexus lesions after experimental traction: a cadaveric study." Journal of Neurosurgery: Spine, **29**(6), pp. 704-710.
- [20] Stouthandel, M. E. J., Vanhove, C., Devriendt, W., De Bock, S., Debbaut, C., Vangestel, C., and Van Hoof, T. 2020. "Biomechanical comparison of Thiel embalmed and fresh frozen nerve tissue." Anatomical Science International, 95(3), pp. 399-407.
- [21] Kawai, H., Ohta, I., Masatomi, T., Kawabata, H., Masada, K., and Ono, K. 1989. "Stretching of the brachial plexus in rabbits." Acta Orthopaedica Scandinavica, 60(6), pp. 635-638.
- [22] Takai, S., Dohno, H., Watanabe, Y., Yoshino, N., Ogura, T., and Hirasawa, Y. 2002. "In situ strain and stress of nerve conduction blocking in the brachial plexus." J. Orthop. Res., 20(6), pp. 1311-1314.
- [23] Phillips, J. B., Smit, X., Zoysa, N. D., Afoke, A., and Brown, R. A. 2004. "Peripheral nerves in the rat exhibit localized heterogeneity of tensile properties during limb movement." The Journal of Physiology, **557**(3), pp. 879-887.
- [24] Singh, A., Shaji, S., Delivoria-Papadopoulos, M., and Balasubramanian, S. 2018. "Biomechanical Responses of Neonatal Brachial Plexus to Mechanical Stretch." Journal of Brachial Plexus and Peripheral Nerve Injury, 13(1), pp. e8--e14.
- [25] Polcaro, L., Charlick, M., and Daly, D. T. 2020. Anatomy, Head and Neck, Brachial Plexus.
- [26] Castaldo, J. E., and Ochoa, J. L. 1984. "Mechanical injury of peripheral nerves. Fine structure and dysfunction." Clin Plast Surg, **11**(1), pp. 9-16.
- [27] Quan, D., and Bird, S. J. 1999. "Nerve conduction studies and electromyography in the evaluation of peripheral nerve injuries." Univ Pa Orthop J, **12**, pp. 45-51.
- [28] Topp, K. S., and Boyd, B. S. 2006. "Structure and biomechanics of peripheral nerves: nerve responses to physical stresses and implications for physical therapist practice." Physical therapy, **86**(1), pp. 92-109.
- [29] Bueno, F. R., and Shah, S. B. 2008. "Implications of tensile loading for the tissue engineering of nerves." Tissue Engineering Part B: Reviews, **14**(3), pp. 219-233.
- [30] Martins, R. S., Bastos, D., Siqueira, M. G., Heise, C. O., and Teixeira, M. J. 2013. "Traumatic injuries of peripheral nerves: a review with emphasis on surgical indication." Arq. Neuro-Psiquiatr., **71**(10), pp. 811-814.
- [31] Somashekar, D., Yang, L. J. S., Ibrahim, M., and Parmar, H. A. 2014. "High-Resolution MRI Evaluation of Neonatal Brachial Plexus Palsy: A Promising Alternative to Traditional CT Myelography." American Journal of Neuroradiology, 35(6), pp. 1209-1213.
- [32] Grewal, R., Xu, J., Sotereanos, D. G., and Woo, S. L. 1996. "Biomechanical properties of peripheral nerves." Hand Clin, **12**(2), pp. 195-204.
- [33] Huang, Y.-G., Chen, L., Gu, Y.-D., and Yu, G.-R. 2011. "Undeveloped semiconic posterosuperior ligament and susceptibility to avulsion of the C-7 spinal nerve in Erb palsy." Journal of Neurosurgery: Pediatrics, **7**(6), pp. 676-680.
- [34] Barberio, C. G., Chaudhry, T., Power, D. M., Tan, S., Lawless, B. M., Espino, D. M., and Wilton, J. C. 2019. "Towards viscoelastic characterisation of the human ulnar nerve: An early assessment using embalmed cadavers." Medical Engineering and Physics, **64**(2019), pp. 15--22.
- [35] Papagiannis, G., Triantafyllou, A., Stasi, S., Yiannopoulou, K. G., Papathanasiou, G., Mitsiokapa, E., Papadopoulos, E. C., Papagelopoulos, P. J., and Koulouvaris, P. 2020. "Biomechanical Behavior and Viscoelastic Properties of Peripheral Nerves Subjected to Tensile Stress: Common Injuries and Current Repair Techniques." Critical Reviews™ in Physical and Rehabilitation Medicine, **32**(3),

- [36] Ozkaya, N., Nordin, M., Goldsheyder, D., and Leger, D. 2012. *Fundamentals of biomechanics*. Springer.
- [37] Sunderland, S., and Bradley, K. 1961. "Stress-strain phenomena in human peripheral nerve trunks." Brain, **84**(1), pp. 102-119.
- [38] Wolff, K. D., Kesting, M., Mücke, T., Rau, A., and Hölzle, F. 2008. "Thiel embalming technique: a valuable method for microvascular exercise and teaching of flap raising." Microsurgery, **28**(4), pp. 273-278.
- [39] Reddy, R., Iyer, S., Pillay, M., Thankappan, K., and Ramu, J. 2017. "Soft embalming of cadavers for training purposes: Optimising for long-term use in tropical weather." Indian J Plast Surg, 50(1), pp. 29-34.
- [40] Zilic, L., Garner, P. E., Yu, T., Roman, S., Haycock, J. W., and Wilshaw, S. P. 2015. "An anatomical study of porcine peripheral nerve and its potential use in nerve tissue engineering." Journal of anatomy, **227**(3), pp. 302-314.
- [41] Mohiuddin, M., Rahman, M., Alim, M., Kabir, M., and Kashem, M. 2011. "Macro anatomical investigation of brachial plexus of the White New Zealand rabbit (Orycotolagus cuniculus)." International Journal of Natural Sciences, 1(3), pp. 74-76.
- [42] Ribitsch, I., Baptista, P. M., Lange-Consiglio, A., Melotti, L., Patruno, M., Jenner, F., Schnabl-Feichter, E., Dutton, L. C., Connolly, D. J., Van Steenbeek, F. G., Dudhia, J., and Penning, L. C. 2020. "Large Animal Models in Regenerative Medicine and Tissue Engineering: To Do or Not to Do." Frontiers in Bioengineering and Biotechnology, 8,
- [43] Chater, M., Camfield, P., and Camfield, C. 2004. "Erb's palsy Who is to blame and what will happen?" Paediatrics & child health, **9**(8), pp. 556-560.
- [44] Singh, A. 2017. "Extent of impaired axoplasmic transport and neurofilament compaction in traumatically injured axon at various strains and strain rates." Brain injury, 31(10), pp. 1387-1395.
- [45] Singh, A., Lu, Y., Chen, C., and M Cavanaugh, J. 2006. "Mechanical properties of spinal nerve roots subjected to tension at different strain rates." J. Biomech., 39(9), pp. 1669-1676.
- [46] Mahan, M. A., Yeoh, S., Monson, K., and Light, A. 2019. "Rapid stretch injury to peripheral nerves: biomechanical results." Neurosurgery, **85**(1), pp. E137-E144.
- [47] Gonik, B., Zhang, N., and Grimm, M. J. 2003. "Prediction of brachial plexus stretching during shoulder dystocia using a computer simulation model." American Journal of Obstetrics & Gynecology, 189(4), pp. 1168-1172.
- [48] Allen, R., Cha, S., Kranker, L., Johnson, T., and Gurewitsch, E. 2005. "Are there differences in mechanical fetal response between routine and shoulder dystocia deliveries?" American Journal of Obstetrics & Gynecology, **193**(6), pp. S38.
- [49] Grimm, M. J., Costello, R. E., and Gonik, B. 2010. "Effect of clinician-applied maneuvers on brachial plexus stretch during a shoulder dystocia event: investigation using a computer simulation model." American journal of obstetrics and gynecology, **203**(4), pp. 339. e331-339. e335.
- [50] Yamada, H., and Evans, F. G. 1970. "Strength of biological materials."
- [51] Anderson, M., Youngner, S., Smith, R. D., Nandyal, R. R., Orlowski, J. P., Jessie Hill, B., and Barsman, S. G. 2020. "Neonatal Organ and Tissue Donation for Research: Options Following Death by Natural Causes." Cell Tissue Bank, **21**(2), pp. 289-302.
- [52] Hanna, A. S., Hellenbrand, D., Schomberg, D., Salamat, S. M., Loh, M., Wheeler, L., Hanna, B., Ozaydin, B., and Shanmuganayagam, D. 2020. "Brachial Plexus Anatomy of Miniature Swine Compared to Human."

- [53] Allen, R., Sorab, J., and Gonik, B. 1991. "Risk factors for shoulder dystocia: an engineering study of clinician-applied forces." Obstet Gynecol, **77**(3), pp. 352-355.
- [54] Rydevik, B. L., Kwan, M. K., Myers, R. R., Brown, R. A., Triggs, K. J., Woo, S. L. Y., and Garfin, S. R. 1990. "An in vitro mechanical and histological study of acute stretching on rabbit tibial nerve." J. Orthop. Res., **8**(5), pp. 694-701.

Table Caption List

Table 1	Summary of in vitro adult human cadaveric BP biomechanical properties [14-20]
Table 2	Summary of in vitro animal BP biomechanical properties [21-22].
Table 3	Summary of in vitro neonatal animal BP biomechanical properties [24].

Table 1

Table 1	Authors	Tissue Type	Mechanical Findings						
	Destandau	BP nerve root		Average Failure Force Avulsion: 69.3 N (29.4–147.1N)					
	et al., 1986	BP nerve root		Rupture: 79.3 N	(39.2–147.1N)		600 mm/min		
	Ma et al., 2013	BP terminal nerve	Мо	dulus of median nerve	higher than ulnar ner	ve	3 mm/min		
Effect of Loading Rate	Marani et al., 1993	BP nerve		At lower rates, nerves elongated to 1/3 their resting length, while at faster rates, nerve elongation was reduced by 1/30 to 1/20 of their resting length					
			Loading Direction	Average Failure Force	Average Failure Strain	Average Failure Stress			
_	Zapalowicz et al., 2000	Intact BP complex	Lateral	388.5 N (217.7–546.3N)	38.6% (19.6%-58.8%)	2.6MPa (1.3-3.5 MPa)	10 mm/min		
of ectio	Zapalowicz et al., 2005	Intact BP complex		630.0 N (365.0-807.0N)	37.0% (23.0%-53.5%)		200 mm/min		
Effect of Loading Direction			45° caudal	665.0 N (563.0-804.0N)					
	Zapalowicz	Intact BP	Perpendicular	558.0 N (365.0-719.0N)			200 mm/min		
ے	et al., 2018	Complex		(555.5 : 15.5.1)					
2	et al., 2018	Complex	Parallel	632.0 N (468.0-757.0N)					

			Failure Stress		
Effect of Fixation	Marani et al., 1993	Fixed BP nerves	0.25 MPa	10 mm/min, 20 mm/min,	
		993 Unfixed BP nerves	0.14 MPa	50 mm/min, 500 mm/min	
			Average Young's Modulus		
	Stoutlandel et al., 2020	Thiel-Fixed andel BP nerves	7.45 ± 3.40 MPa	0.059//202	
		Unfixed BP nerves	9.20 ± 1.20 MPa	0.05%/sec	

Table 2

	Authors	Species	Tissue Type	Mechanical Findings				Loading Rate
				Average	Failure Stress	Average F	ailure Strain	
	Kawai	Rabbit	C6 nerve root C6	Avulsion: 26	MPa (23-27 MPa)		9%	500
	Let al., 1989	nerve root	Rupture: 46 MPa (44–49 MPa)		7%		mm/min	
				Average Maximum Tensile Force	Average Ultimate Tensile Stress	Average Ultimate Strain	Average Elastic Modulus	
	Takai et al., 2002	Rabbit	Lower BP trunk	16.9 ± 2.7 N	6.9 ± 0.13 MPa	24.0 ± 1.1%	28.5 ± 1.8 MPa	10 mm/min
					Average Stiffr	ness Ratio ^a		
Effect of Loading Direction	Phillips et al., 2004	Rat	Median		0.5 ± (0.07		10 mm/min
				Loading Direction	Avera	ge Failure Fo	rce	
	Kawai et al., 1989	Rabbit	Intact BP complex	Upward Lateral Downward	Lateral 23 N (19–31 N)			500 mm/min

^a Stiffness Ratio = joint stiffness/non-joint stiffness

Table 3

	Authors	Species	Tissue Type	Mechanical Findings				
of Rate				Average Maximum Force	Average Maximum Stress	Average Strain	Average E	
Effect Loading	Singh et al., 2018	Singh Piglet con	BP	1.83 ± 0.14 N	0.56 ± 0.07 MPa	32.0 ± 3.0%	2.87 ± 0.32 MPa	0.6 mm/min
			complex	3.52 ± 0.42 N	1.15 ± 0.15 MPa	32.0 ± 2.0%	5.27 ± 0.69 MPa	600 mm/min

Figure Captions List

Fig. 1 Schematic of brachial plexus anatomy. MSC: Musculocutaneous, C: Cervical, Th: Thoracic.

- Fig. 2 Classification of brachial plexus injury observed by the degree of damage of neural structures (i.e., axon, myelin sheath) and connective tissue structures (i.e., epineurium, perineurium, endoneurium). (A) Normal. (B) Neuropraxia characterized by injury to the myelin sheath (pink). (C) Axonotmesis characterized by injury to both axon and myelin sheath (dashed line and pink, respectively). (D) Neurotmesis characterized by injury to the axon, myelin sheath, and surrounding connective tissue structures (dashed line, pink, and gap with red thunderbolt, respectively).
- Fig. 3 (A) Summary of search results using keywords. (B) Flow chart of process utilized for selection of studies included in this review article.
- Fig. 4 Representative failure (A) load-elongation and (B) stress-strain curves from a tensile test of a rabbit tibial nerve. Figure modified from Ref. [37].
- Fig. 5 (A) Schematic of testing set-up to stretch BP spinal nerve roots (i.e., Th1) from fresh adult human cadavers until failure at a rate of 600 mm/min. The end of the BP spinal nerve roots was clamped on the moving end of the testing set-up. (B) Average rupture force [N] of each BP spinal nerve roots [14]. C: cervical, Th, Thoracic.

- Fig. 6 Bar graphs detailing (A) total number of avulsion and non-avulsion injury-types and (B) average rupture force of total avulsed and non-avulsed BP spinal nerve roots stretched at 600 mm/min until failure [14].
- Fig. 7 Bar graph detailing (A) individual BP spinal nerve root avulsion and non-avulsion injury-types and (B) average rupture force of each BP spinal nerve roots stretched at a rate of 600 mm/min until failure [14]. C: Cervical. Th: Thoracic.
- Fig. 8 Bar graph detailing number and type of initial injury-type of intact BP with respect to loading direction [17].
- Fig. 9 (A) Loading directions of 45° caudal (Group A), perpendicular (Group B), and parallel (Group C) with respect to the spinal column applied to fresh intact adult human cadaveric BP complexes at a rate of 200 mm/min. The BP terminal branches were clamped on the moving end of the testing setup. Figure modified from [19]. (B) Average maximum force of the intact BP complexes for each group.
- Fig. 10 Bar graphs detailing (A) the nerve root avulsed with respect to loading direction (Group A: 45° caudal, Group B: perpendicular, Group C: parallel); and (B) the site of injury of rupture-type injuries with respect to loading direction (Group A: 45° caudal, Group B: perpendicular, Group C: parallel) [19].
- Fig. 11 (A) Average Young's modulus of the median nerve, a BP terminal nerve. (B) Representative biomechanical response of Thiel fixed (gray) and unfixed (black) median nerve stretched at a strain rate of 0.5%/sec. Figure modified from Ref. [20].

Fig. 12 Average failure force of intact BP complex with respect to loading direction stretched at a rate of 500 mm/min [21].

Fig. 1

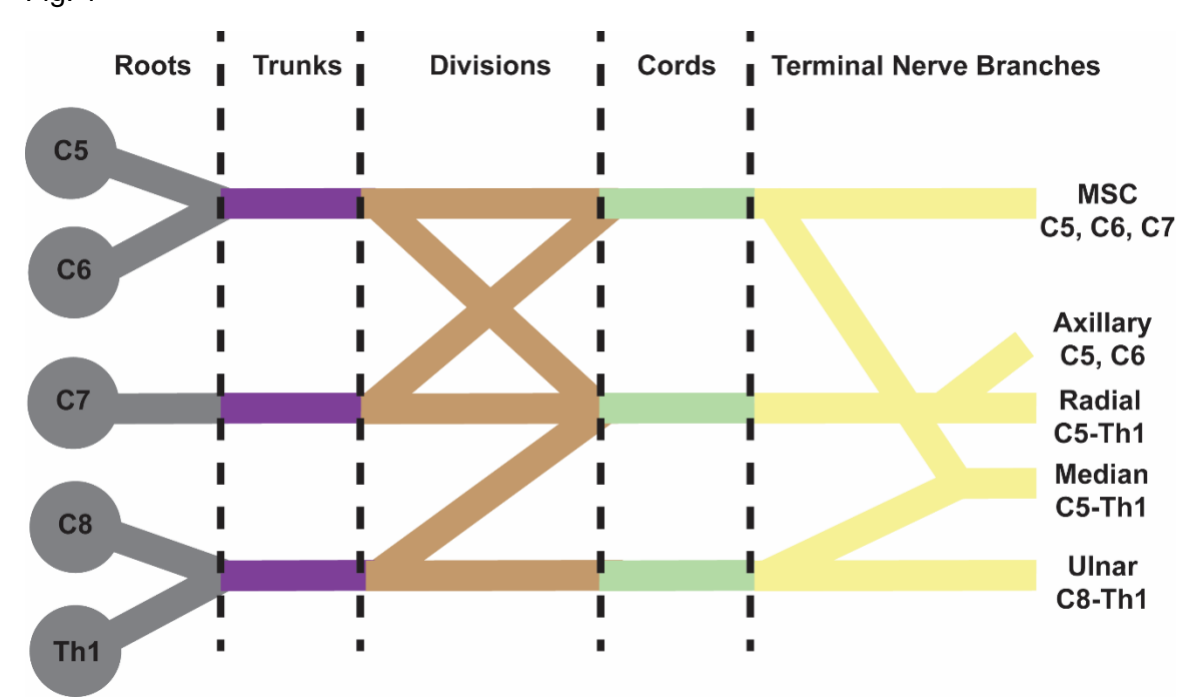


Fig. 2

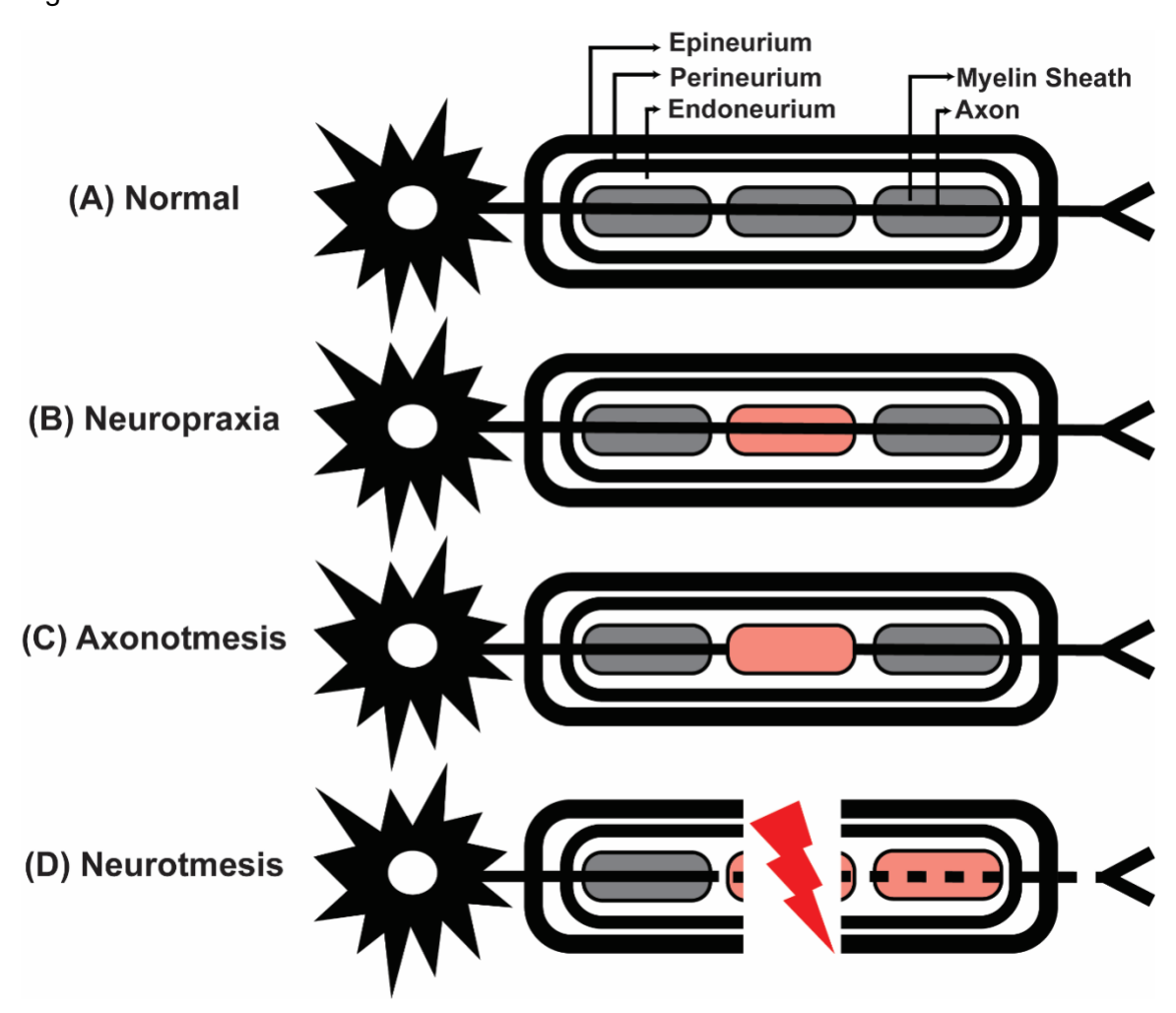


Fig. 3

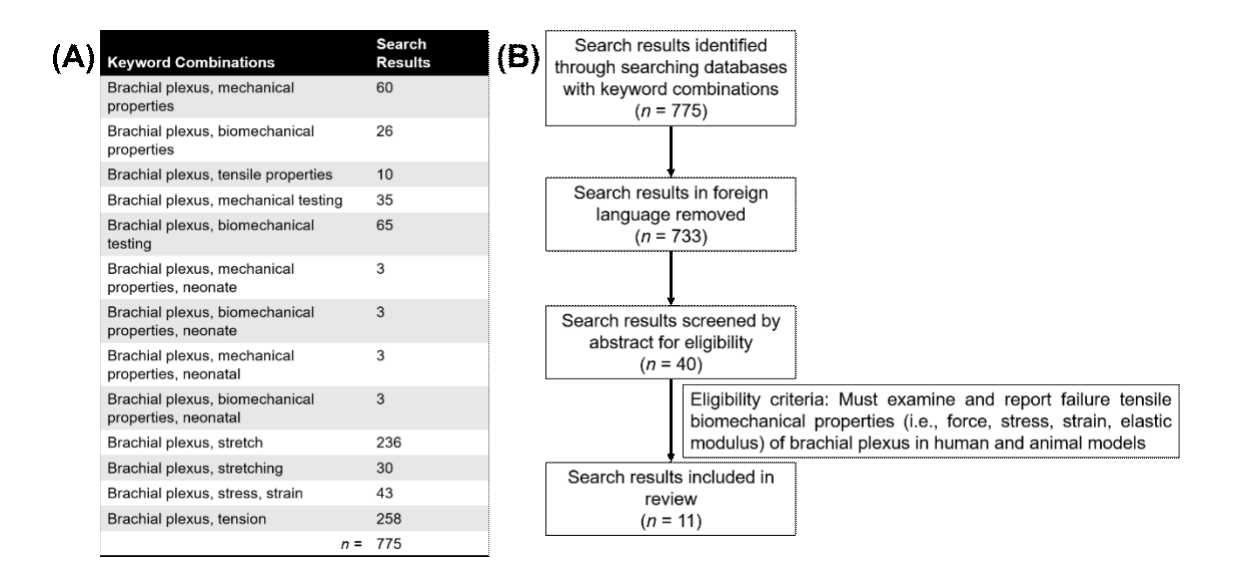


Fig. 4

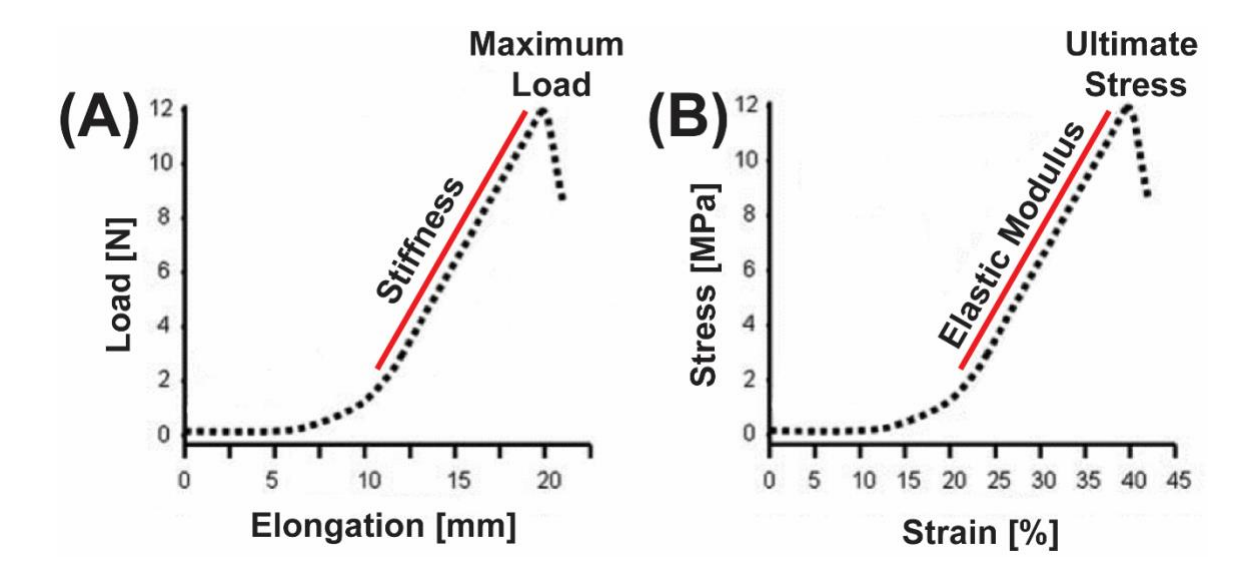
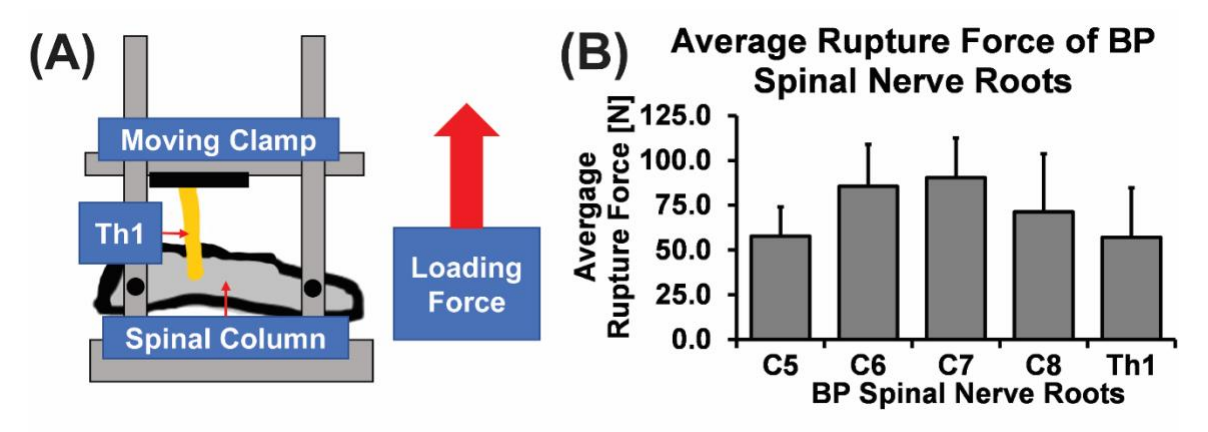


Fig. 5



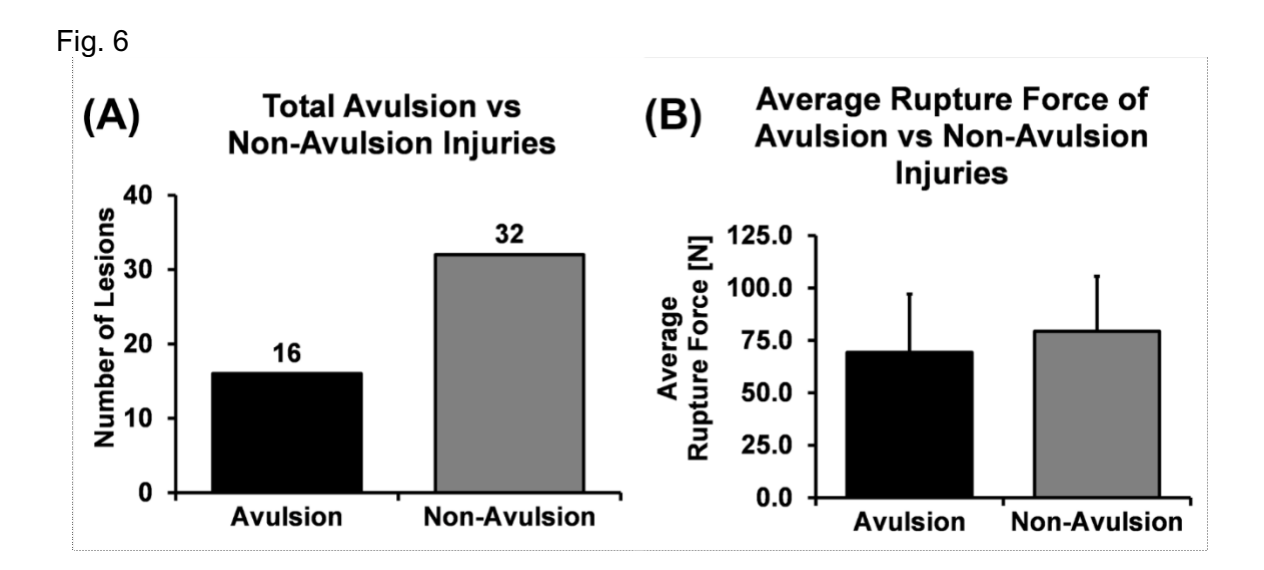
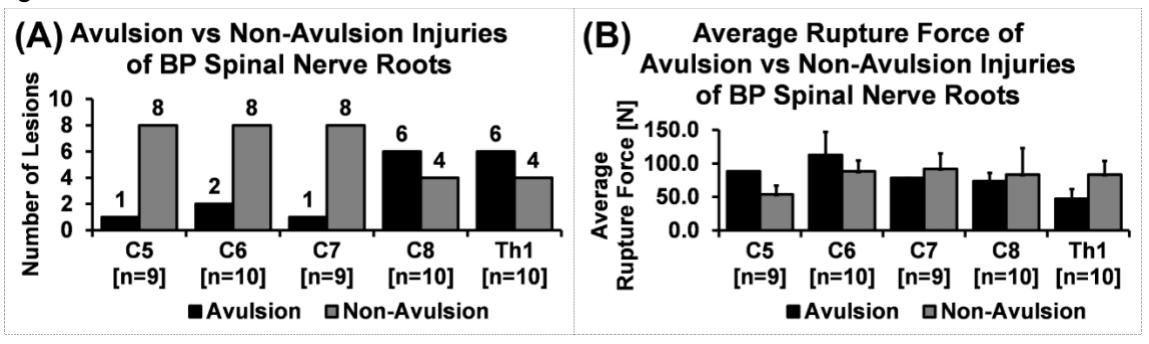
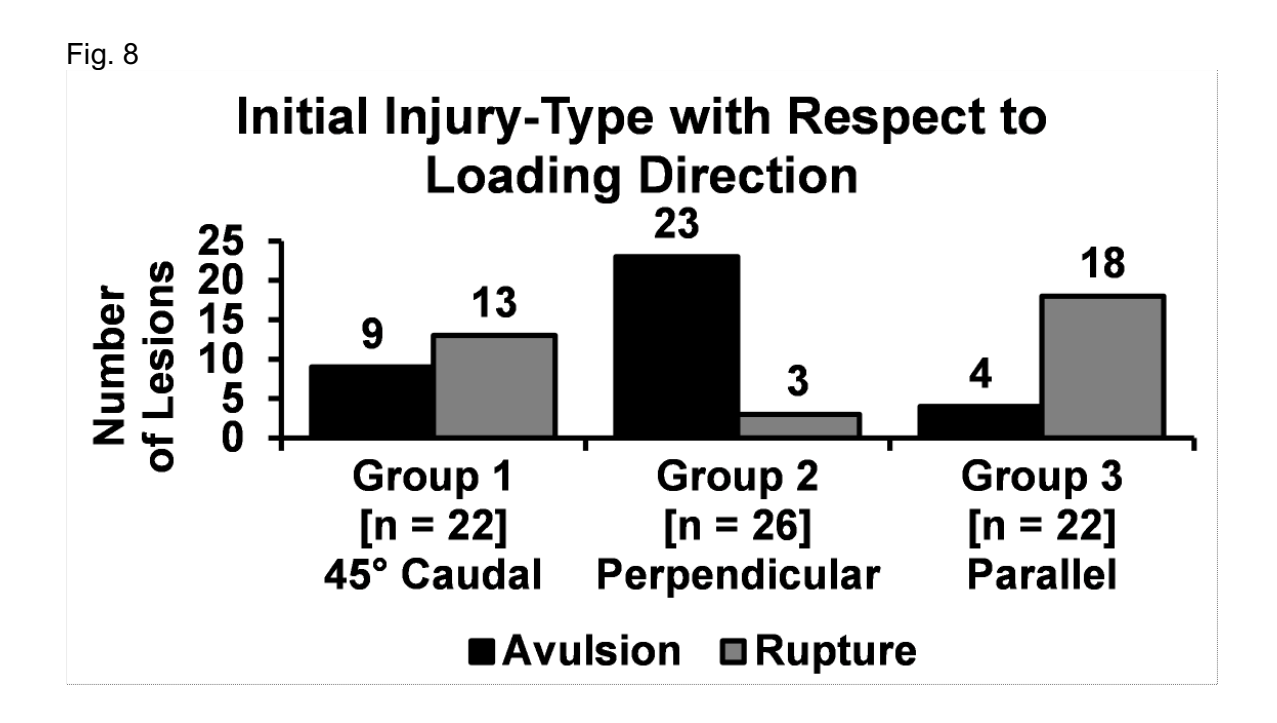


Fig. 7





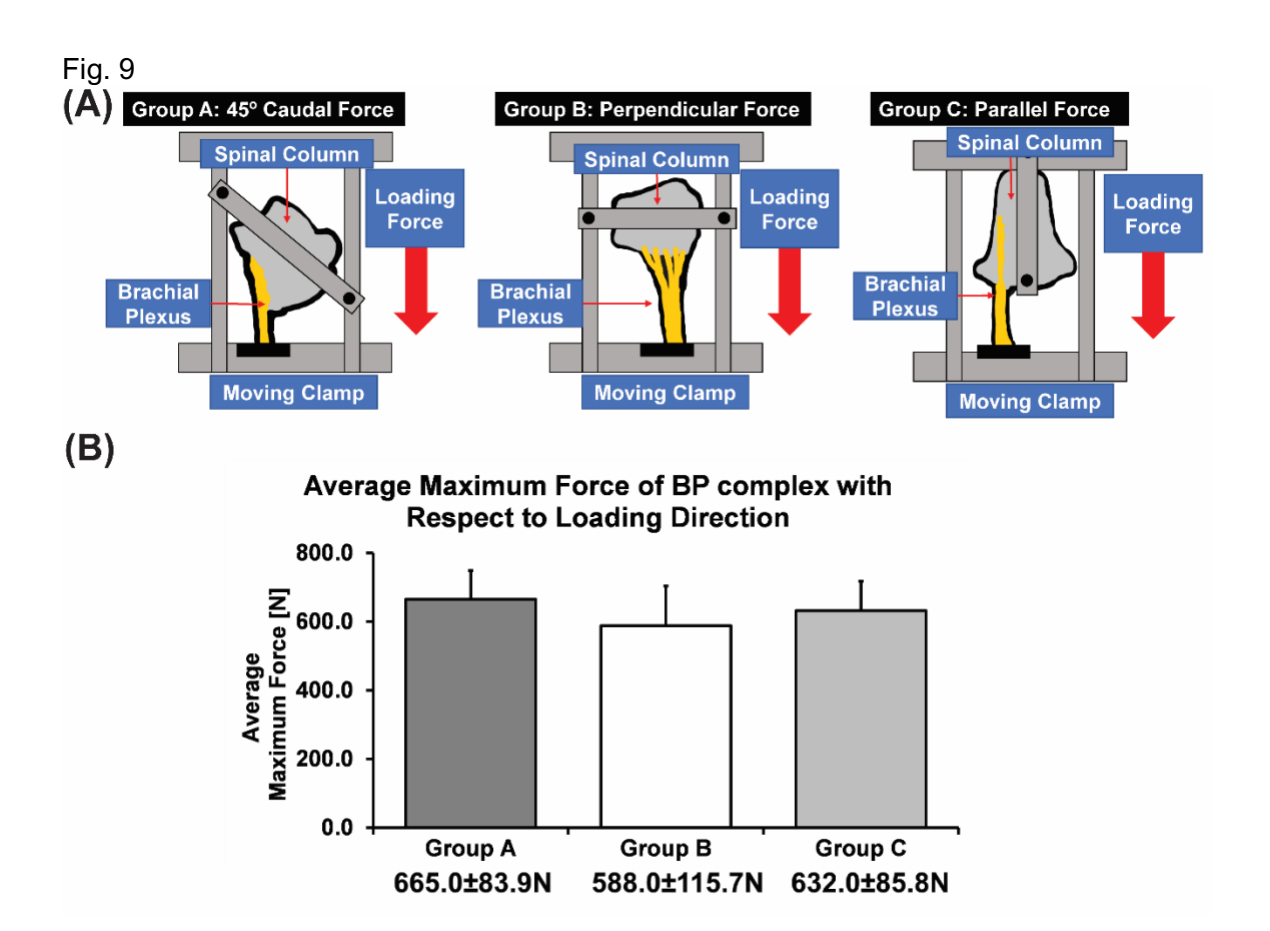


Fig. 10

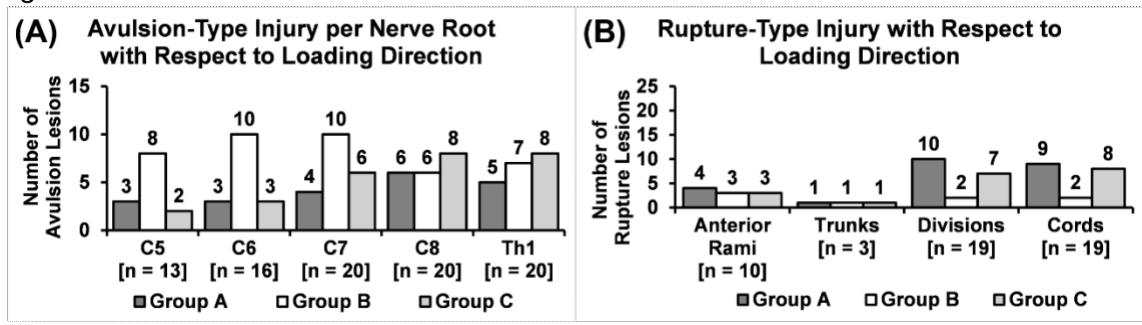


Fig. 11

